

Proposal for III-V ordered alloys with infrared band gaps

Su-Huai Wei and Alex Zunger
Solar Energy Research Institute, Golden, Colorado 80401

(Received 21 February 1991; accepted for publication 5 April 1991)

It is shown theoretically that the recently observed spontaneous ordering of III-V alloys that yields alternate monolayer (111) superlattices provides the opportunity for achieving infrared band gaps in systems such as $(\text{InAs})_1(\text{InSb})_1$ and $(\text{GaSb})_1(\text{InSb})_1$. A substantial reduction in the *direct* band gap is predicted to result from the *L*-point folding that repel the Γ band-edge states.

Substantial effort has recently been focused on developing semiconductor materials for infrared (IR) devices in the wavelength range above 8 μm . In addition to the need of intersubband absorption in tunnelling III-V superlattices,² four general physical principles have been previously utilized to directly shift band gaps into the IR spectral

(i) *Bulk alloying*. In this simple approach one uses the fact that alloy band gaps vary smoothly and continuously with composition (often with a parabolic deviation from linearity), and seeks a combination of mutually soluble CdTe) semiconductors that produces a $(\text{SG})_{1-x}(\text{LG})_x$ alloy with a desired IR gap.

(ii) *Superlattice quantum confinement without strain*. The basic idea here is to take a semiconductor with a very large gap (LG) and a small lattice constant (SG), and to alternate it with a semiconductor with a smaller gap (LG) and a larger lattice constant (LGLL). For small layer thicknesses (p, q), quantum confinement effects in the smaller gap (SGSL) raise the conduction band minimum (CBM), thus increasing the superlattice gap above that of pure SG.

LG = CdTe by Schulman and McGill³ and by Smith *et al.*⁴ and examined experimentally, e.g., by Reno and Faurie.⁵

(iii) *Superlattice strain-induced band-gap shift*. A semiconductor with a smaller gap and small lattice constant (SGSL) and layer it coherently with a material having a larger gap and larger lattice constant (LGLL), forming a strained-layer (SGSL)_p / (LGLL)_q superlattice. Coherence of SGSL with LGLL

interface, thus lowering its Γ conduction-band minimum. At the same time, tetragonal *compression* of SGSL in the perpendicular direction splits its VBM, raising the energy of the upper split components. Both effects act to reduce the band gap.

Since quantum confinement effects at small (p, q) act in the opposite direction, increasing the band gap, relatively thick layers are required to achieve the desired band gap.

herently the misfit strain limits the maximum thickness that can be used.

(iv) *Superlattice-induced band inversion*. The basic

of the constituents (AC) is lower in energy than the VBM of the other (BC); in this type of band lineup, the superlattice band gap is determined by the relative energy of the constituents. This approach has been proposed by Arch *et al.*⁸ for AC = InAs and BC = GaSb. Like in (iii) above, here, too, relatively thick layer would be required to counteract

"II" band arrangement, thick layers deteriorate severely the intensity of optical absorption due to increased separation between electrons and holes. To reduce the layer thickness needed, the principle of "strain-induced band-gap reduction" has been proposed by Mailhot⁹ for AC = InAs and BC = Ga_{1-x}In_xSb. This system was grown successfully by Chow *et al.*¹⁰ where far-infrared photoluminescence was observed.

We discuss here a different principle of achieving infrared band gaps with III-V materials, namely "band-gap reduction by *L*-point folding". In a typical III-V alloy (e.g., GaAs), the Γ conduction-band minimum (CBM) and the Γ valence-band maximum (VBM) are at the Brillouin zone center. This leads to a

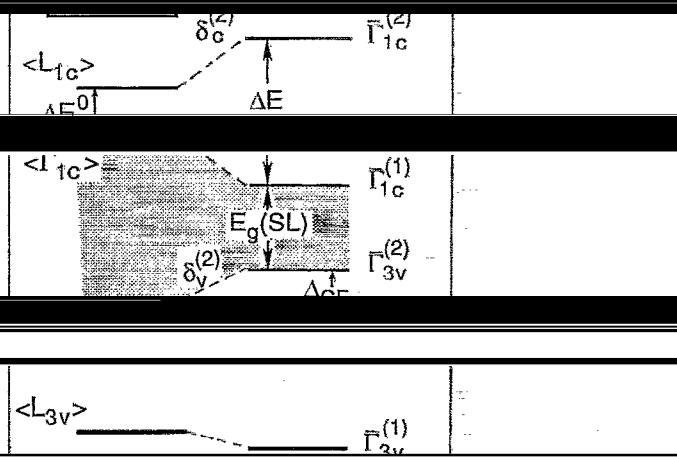


FIG. 1. Schematic plot of energy level shift at Γ of a typical III-V alloy forming a Γ -like structure. States with same nomenclature in the same diagram are degenerate.

TABLE I. Calculated energy differences (eV) between the repelling states $\langle L_{1c} \rangle$ and $\langle \Gamma_{1c} \rangle$ before (ΔE^0) and after (ΔE) the perturbation potential is turned on. Values in parenthesis are for unrelaxed structures.

	GaAs/InAs	GaAs/InSb	GaAs/GaSb	InAs/InSb
$\Delta E^0 = \langle L_{1c} \rangle - \langle \Gamma_{1c} \rangle$	0.99	0.68	0.47	1.0
$\Delta E = \bar{\Gamma}_{1c}^{(2)} - \bar{\Gamma}_{1c}^{(1)}$	1.43 (1.22)	1.22 (1.02)	1.77 (1.28)	1.84 (1.39)
$R = \Delta E - \Delta E^0$	0.44 (0.23)	0.54 (0.34)	1.30 (0.81)	0.84 (0.39)

reduces the direct band gap, thus overwhelming the opposite

ence between the superlattice states $\bar{\Gamma}_{1c}^{(2)}$ and $\bar{\Gamma}_{1c}^{(1)}$. Table I

also the difficulties with misfit dislocations and with con-

approximation (LDA), as implemented by the semirelativistic linearized augmented plane-wave (LAPW) method.¹⁵

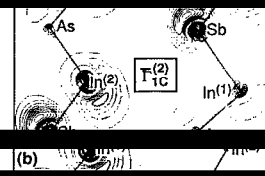
It has recently been noted¹⁴ that numerous III-V alloys exhibit in vapor phase growth *spontaneous* long-range ordering in the form of monolayer (AC)₁/(BC)₁ superlattices in the (111) orientation (the "CuPt-like structure"). The degree of ordering is generally maximized in certain growth temperature ranges and sub-

In all cases we have assumed that the superlattice is matched to a substrate whose lattice constant is the average of its constituents. Table I reveals a substantial contribution to R. This can be exemplified by the results for

CuPt ordering are given in Ref. 12. In all cases, ordering occurred as a result of *homogeneous* alloy growth *without*

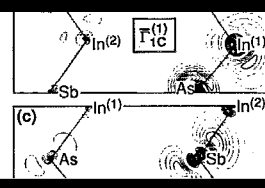
contribution to R. This can be exemplified by the results for

point are constructed from the zincblende-like states at $\langle \Gamma \rangle + \langle L^{111} \rangle$. The folded zincblende states at this wave vector are coupled in the superlattice by the perturbing potential $\delta V(\mathbf{r}) = \delta V^{(\text{chem})} + \delta V^{(\text{size})}$ that has the symmetry Γ_{1c} .



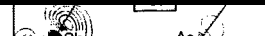
As	0.003	0.014
In ⁽¹⁾	0.023	0.071
Sb	0.350	0.086
In ⁽²⁾	0.453	0.012

size mismatch. This potential couples the alloy states and leads to a "level repulsion" between them, whereby superlattice states are displaced relative to the unperturbed (virtual crystal) states. For example, the $\bar{\Gamma}$ -folding alloy states $\langle \Gamma_{1c} \rangle$ and $\langle L_{1c} \rangle$ couple through δV , producing the superlattice states $\bar{\Gamma}_{1c}^{(1)}$ and $\bar{\Gamma}_{1c}^{(2)}$ that are lowered and raised



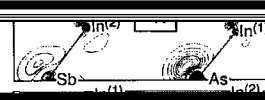
Sb	0.120	0.001
In ⁽²⁾	0.088	0.014

The lowering of the CBM will be denoted (Fig. 1) as



As	0.000	0.190
In ⁽¹⁾	0.000	0.010

produce the superlattice states Γ_{3v} and Γ_{3v} that are also mutually repelled (Fig. 1). The increase in the energy of the VBM will be denoted (Fig. 1) as $\delta^{(2)} = -\epsilon(\Gamma_{1c})$



Sb	0.020	0.000
In ⁽²⁾	0.020	0.076

mum at X is considerably higher in these systems¹⁴ than $\bar{\Gamma}_{1c}^{(1)}$, the former will not be discussed here.



FIG. 2. Charge density distribution $\rho(\mathbf{r})$ and $\bar{\Gamma}_{1c}^{(1)}$ and $\bar{\Gamma}_{1c}^{(2)}$ in (InAs)₁(InSb)₁ in CuPt-like structure, plotted in the (110) plane. The contour step size is $4 \times 10^{-3} e/\text{au}^3$. Charges are normalized to $2 e/\text{cell}$. On the right hand side we also give the angular momentum and site decomposed charge (in units of e) for these states, where In⁽¹⁾ and In⁽²⁾

To quantify the extent of level repulsion, we denote by ΔE^0 the $\langle L_{1c} \rangle - \langle \Gamma_{1c} \rangle$ energy difference *before* coupling

TABLE II. Experimental low-temperature (LT) band gaps for the binary constituents and our predicted semirelativistic LDA-corrected low-temperature direct band gaps [Eq. (4)] for the four systems forming CuPt-like structure. The numbers in parenthesis are crystal field (denoted Δ_{CF} in Fig. 1) averaged values. The last row gives the change in the spin-orbit splitting $\delta\Delta_0$ relative to their respective averaged binary values. To include spin-orbit interactions, subtract 1/3 $\delta\Delta_0$ from $E_g(\text{SL})$. All energies are in eV.

	GaAs/InAs	GaSb/InSb	GaAs/InSb	InAs/InSb
$E_g(\text{binary})^a$	1.52/0.42	0.81/0.24	1.52/0.81	0.42/0.24
$E_g(\text{SL})^b$	0.55 (0.58)	0.09 (0.12)	0.27 (0.36)	-0.28 (-0.20)
$\delta\Delta_0$	-0.01	-0.01	0.08	0.08

InAs/InSb: we find that without structural relaxation [where $\delta V(\mathbf{r}) = \delta V^{(\text{chem})}(\mathbf{r})$] band coupling gives $R = 0.39$ eV, while after relaxation $\delta V^{(\text{size})}(\mathbf{r})$ further increases R by an additional 0.45 eV.

the various states, as illustrated in Fig. 2 for (InAs)₁/(InSb)₁. We see that each member of a pair of coupling states ($L_{1c} + L_{1c}$ or $L_{1c} + L_{1c}$) has its charge localized on the In-As bonds, while the wave functions are localized on the In-As bonds.

valence-band maximum $\Gamma_{3p}^{(2)}$ is found to be localized systematically on the heavy atom semiconductor, while the conduction band minimum $\Gamma_{1c}^{(1)}$ is localized on the light atom semiconductor.

strength of the VBML-LBML optical transition is predicted to be very strong.

As repeat periods are very short, we find that relaxation enhances substantially both the wave function localization and the mixing of s character into the valence-band-edge states [Fig. 2(d)] that are pure p states in the cubic binary constituents. This affects the spin-orbit splitting Δ_{SO} . Our predicted changes in the spin-orbit splitting are given in Table II. It shows that in the common-anion systems $\delta\Delta_0 \lesssim 0$, while for common-cation systems the negative bowing ($\delta\Delta_0 > 0$) is sizable.

dicted SL gap" $E_g(\text{SL})$ by subtracting the calculated level shifts (Fig. 1) from the experimental¹⁶ (exptl) average of the gaps of the constituents

This is a reasonable approximation for the LDA-corrected band gaps.

the lattice constant of the SL is larger than the other constituent. Consider

(iii) above would therefore suggest that these SL's will have a larger band gap than the bulk constituent with the smaller lattice constant. Table II shows, however, that in all cases except

strong level repulsion that overwhicms other effects. The

ergy denominators¹¹ ΔE^0 (Table I), consistent with a perturbation theory description. Indeed, since the L_{1c} level is closer in most alloys to Γ_{1c} than is X_{1c} , the level repulsion R in (111) SL's is larger than in (001) SL's.

Our semirelativistic calculations predict that in the perfectly ordered CuPt-like structure (GaAs)₁(InSb)₁ and (InAs)₁(InSb)₁ will have direct band gaps of 0.09 and 0.12 eV, respectively, while the other two systems are not perfectly ordered. For example, for

given composition x one has additional control over the band gap through variations of the growth parameters that

This work was supported in part by the U.S. Department of Energy.

¹See reviews by R. Triboulet, *Semicond. Sci. Technol.* **5**, 1073 (1990) and in *Materials for Infrared Detectors and Sources*, edited by R. F. C. Barrow, J. E. Schatzne, and J. T. Cheung (Materials Research Society, Pittsburgh, 1987), Vol. 90.

²J. N. Schulman and T. C. McGill, *Appl. Phys. Lett.* **34**, 663 (1979).

⁴D. L. Smith, T. C. McGill, and J. N. Schulman, *Appl. Phys. Lett.* **43**, 180 (1983).

⁵J. Reno and J. P. Faurie, *Appl. Phys. Lett.* **49**, 409 (1986).

Stein, *Appl. Phys. Lett.* **52**, 831 (1988).

⁸D. K. Arch, G. Wicks, T. Tonaue, and J.-L. Staudenmann, *J. Appl. Phys.* **58**, 3933 (1985).

⁹D. L. Smith and C. Mailhot, *J. Appl. Phys.* **62**, 2545 (1987); C. Mailhot and D. L. Smith, *J. Vac. Sci. Technol. A* **7**, 445 (1989).

Sci. Technol. **B 8**, 710 (1990).

¹¹J. N. Schulman, *Appl. Phys. Lett.* **34**, 663 (1979).

J. T. McDermott, K. G. Reid, N. A. Elmashry, S. M. Bedair, W. M. Dueser, Y. Yin, and F. H. Bahle, *Appl. Phys. Lett.* **56**, 1172 (1990).

S.-H. Wei and H. Krakauer, *Phys. Rev. Lett.* **55**, 1200 (1985).

¹⁶*Landolt-Bornstein: Numerical Data and Functional Relationships in Science and Technology*, edited by O. Madelung, M. Schulz, and H. Weiss (Springer, Berlin, 1982), Vol. 17a.

binary constituents (Table II) and $b \approx 0.6$ eV (Ref. 16) is the bowing